Journal of
Ship&Ocean
Technology
©MARCH 2008

SOTECH Vol. 12, No. 1, pp. 1 ~ 15, 2008

Numerical Simulation of Edgetone Phenomenon in Flow of a Jet-edge System Using Lattice Boltzmann Model

Ho-Keun Kang[1]

[1] Research and Development Center, Korean Register of Shipping, Daejeon, Korea;
Corresponding Author: hkkang@krs.co.kr

Abstract

An edgetone is the discrete tone or narrow-band sound produced by an oscillating free shear layer, impinging on a rigid surface. In this paper, 2-dimensional edgetone to predict the frequency characteristics of the discrete oscillations of a jet-edge feedback cycle is presented using lattice Boltmznan model with 21 bits, which is introduced a flexible specific heat ratio γ to simulate diatomic gases like air. The blown jet is given a parabolic inflow profile for the velocity, and the edges consist of wedges with angle 20 degree (for symmetric wedge) and 23 degree (for inclined wedge), respectively. At a stand-off distance w, the edge is inserted along the centerline of the jet, and a sinuous instability wave with real frequency is assumed to be created in the vicinity of the nozzle exit and to propagate towards the downward. Present results presented have shown in capturing small pressure fluctuating resulting from periodic oscillation of the jet around the edge. The pressure fluctuations propagate with the speed of sound. Their interaction with the wedge produces an irrotational feedback field which, near the nozzle exit, is a periodic transverse flow producing the singularities at the nozzle lips.
It is found that, as the numerical example, satisfactory simulation results on the edgetone can be obtained for the complex flow-edge interaction mechanism, demonstrating the capability of the lattice Boltzmann model with flexible specific heat ratio to predict flow-induced noises in the ventilating systems of ship.
Keywords: lattice Boltzmann model, edgetone, flow-induced noise, feed back loop

1 Introduction

In the design of naval or cruise vessels, prediction and reduction of flow noise radiated from the ventilation systems of vessel is of primary important for the reliable operation of onboard acoustic instruments. Because of space constraints, air ducts used aboard ships are often very small and have sharp curves and bends. This results in air moving through the ducts at very high velocities. Air moving at high velocities can be the cause of noise and vibration in the ventilation system. Fans can also project noise throughout the ventilation system if they are poorly mounted, not properly isolated from air ducts, and/or are the

wrong size. Amongst these sources the ventilation noises, particularly for the edgetone, is the unfavorable one for acoustic survey operations since the dominant noise levels can cover a wide frequency band. Therefore the prediction and reduction of ventilation noises for these type of vessels is utmost important.

Edgetone phenomenon, oscillating phenomenon of a jet-edge system is one of the basic flow-induced noises problems. Since the loud noise with the peak frequency is caused by the phenomenon, it is important to clarify the mechanism. Edge tone is a discrete frequency sound produced by several flow geometries in which a free shear layer interacts with a solid boundary as shown in Figure 1. The noise is generated because the impinging jet forms a self-excited flow maintained by a feedback loop. The phenomenon has been investigated by many researchers, for example Brown (1937) who performed detailed experiments regarding four stages of the edgetone. The peak frequency of edgetone called the edgetone frequency which corresponds to the frequency of flow-field oscillation. As the jet velocity or the stand-off distance w is continuously changed, the edgetone frequency basically changes continuously but sometimes changes drastically at the certain conditions. The sudden change of the frequency is called "frequency jump." The frequency jump is caused by the change in oscillation mode (or stage) of the edgetone by the formula:

$$f = 0.466k(U - 40)\left[\frac{1}{w} - 0.07\right] \tag{1}$$

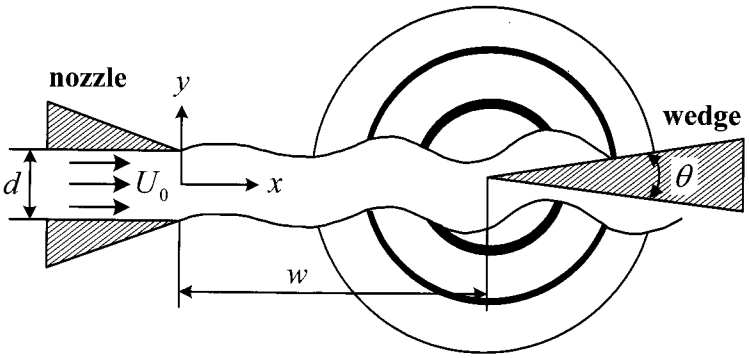

Figure 1: Schematic of the edgetone configuration

where f is the frequency with k=1.0, 2.3, 3.8 and 5.4 for the four stages or fluid dynamic modes, respectively. Particularly obvious are the main features according to the simplifying consideration first stated by Powell (1961). Such a feedback theory was proposed by Rossiter (1962) in the following form

$$\frac{w}{c_p} + \frac{w}{c_0} = \frac{k}{f}, \quad k = 1,2,3,\cdots \tag{2}$$

where w is the stand-off distance, c_p the phase velocity, and c_0 is the acoustical wave. From experiments it appears that k has to be replaced by $(k-\beta)$, β being a phase offset. As a result the above relation would yield

$$S_w = (k-\beta)/(U/c_p + Ma) \tag{3}$$

where $Ma = U / c_0$ is the Mach number. Furthermore, the theoretical developments performed by Holger et al. (1977) and Howe (1998) have confirmed the analogy. Several scaling laws derived from experimental or theoretical work have also been proposed to fit the dependency of the oscillation frequency f on the parameter d/w, where d is the nozzle height. These authors proposed the following more general law in terms of the Strouhal number S_d for $k = 1$:

$$S_d = \frac{f \cdot d}{U} = C \cdot (d/w)^n \tag{4}$$

where n equals 3/2 for the w dependence. In general the constant C might depend also the Reynolds number. In Eq. (4) a positive feedback loop may be formed by more than one value k for a given ratio of k/f. There is one dominant frequency and therefore the frequency jumps at certain distances. Our interest in these simulations is focused on stage I, or the fundamental fluid dynamical mode $k = 1$.

Since it is difficult to verify the feedback loop mechanism of edgetone in experimental approaches, computational methods are expected to clarify the mechanism. Recent numerical simulations on a edge tone and the associated self-sustained flows are reported by Dougherty et al.(1994), Bamber et al.(2004), Deviller and Coutier-Delgosha(2005), and Tsuchida et al.(2006). Due to complicated apparatus-dependent vortex-acoustic interactions, various published experimental and numerical results do not universally agree. Some nozzles have acute lips while others did not. Some jet-wedge systems had little far-field feedback while others apparently have additional acoustic interference due to the supporting casing and other devices. Due to the shape and dimensions of the orifice, the pressure drop and velocity profiles may not have been the same, even under the same flow rates. Consequently, different flow conditions have yielded different frequency responses.

In this study, as a benchmark problem, a fluid dynamical phenomenon of edge tones is simulated. This may result in an oscillatory behavior of the jet due to positive fluid dynamical feedback loop. The phenomenon presented is a fluid dynamical problem which is based on a instability of the flow due to shear layers. Here, as the Reynolds number further increases and surpasses a critical value the system enters into another regime, turbulence becomes dominant (Lesieur 1993). The simulations, therefore, are treated within the regime of instability, but below turbulence. The flow seems to be laminar at small perturbations, but due to the growing instability there is a breakdown of the laminar flow and flow separation occurs. Present simulations deal with Reynolds numbers, $200 \leq \mathrm{Re} \leq 600$ and $0.027 \leq S_t \leq 0.08$, respectively.

2 Numerical method

2.1 Finite difference-based lattice Boltzmann model

As a newly developed numerical method, the lattice Boltzmann (LB) method (Alexander et al. 1993; Chen and Doolen 1998), a novel kinetic–based approach for simulating fluid flow and associated transport phenomena, has been successfully applied since it originated from the lattice gas cellular automata (LGCA) method (Wolfram 1986). Considered an attractive alternative to conventional finite difference schemes because it recovers the Navier – Stokes equations, the LBM is computationally more stable, and easily parallelizable. In traditional numerical methods, the macroscopic variables are obtained by solving the

Navier-Stokes equations. However, the LBM solves the microscopic kinetic equation for particle distribution function from which the particles move at unit speed on a regular grid subject to particle movement and simplified collision rules, which conserve the total fluid mass, momentum and energy.

The numerical solution of flow-induced noise problems at relatively low Mach number flow is still a major problem, which is often seen in various fields of industry. Here, lattice Boltzmann method seems to be the most promising method that computes directly source fluctuations in the flow for the prediction of flow-induced noises, and at the same time the prediction of noise seems to be one of the most appropriate areas of engineering applications of LBM. In the field of flow-induced noises some fundamental studies have been undertaken to show its validity concerning linear and nonlinear wave propagation (Buick et al. 2000), acoustical streaming (Haydock and Yeomans 2001), ultra sound gas flow meter (Wilde 2004), and Aeolian tone and edgetone(Kang et al. 2006; Kang and Tsutahara 2007). Buick et al. (2000) used the technique to simulate linear sound waves when the pressure variations are considered to be a small perturbation. They also extended the scope of the simulation to consider nonlinear waves and showed that the LBM and the incompressible approximation are not limited to the linear regime. Haydoc and Yeoman (2001) reported to simulate the acoustical streaming produced by the interaction of an acoustic wave with a boundary. With comparison to Rayleigh streaming in appropriate limits, they showed how deviations from those limits affect the acoustic streaming. Wilde (2004) also investigated to the problem of a Helmholtz resonator under a grazing flow and to the propagation of sound waves in a turbulent flow in a duct of an ultra sound gas flow meter, showing great potential for the method in the field of flow acoustics. More recently, Kang and Tsutahara (2007) presented an approach to simulate flow-induced noises by modifying the finite difference-based lattice BGK model, demonstrating that their code is much cheaper with respect to the computational cost of the acoustic of DNS (Inoue and Hatakeyama 2002). So the use of the LBM as a tool for computational flow-induced noises can be seen in its early stage.

Table 1: Particles of D2Q21 model

p	k	Velocity vector $\mathbf{c}_{pki}=(c_{pkix},c_{pkiy})$	$c_{pk}=\lvert\mathbf{c}_{pki}\rvert$
0	0	(0,0)	0
1	1	(1,0),(0,1),(-1,0),(0,-1)	1
1	2	(2,0),(0,2),(-2,0),(0,-2)	2
1	3	(3,0),(0,3),(-3,0),(0,-3)	3
2	1	(1,1),(-1,1),(-1,-1),(1,-1)	$\sqrt{2}$
2	2	(2,2),(-2,2),(-2,-2),(2,-2)	$2\sqrt{2}$

The Boltzmann equation governing the velocity distribution function f_i may be written, with single relaxation time ϕ, as:

$$\frac{\partial f_i}{\partial t}+c_{i\alpha}\frac{\partial f_i}{\partial r_\alpha}-ac_{i\alpha}\frac{\partial}{\partial r_\alpha}\frac{f_i-f_i^{(0)}}{\phi}=-\frac{1}{\phi}\left(f_i-f_i^{(0)}\right) \tag{5}$$

Here, the real number f_i is the normalized number of particle at each lattice node and time t, moving direction i, and α represents the Cartesian coordinates, $f_i^{(0)}$ on the RHS is the local equilibrium distribution function, and ϕ is the single relaxation time factor.

$$f_i^{(0)} = F_i\rho\left[1-2B(\mathbf{c}\cdot\mathbf{u})+2B^2(\mathbf{c}\cdot\mathbf{u})^2+B(\mathbf{u}\cdot\mathbf{u})-\frac{4}{3}B^3(\mathbf{c}\cdot\mathbf{u})^3-2B(\mathbf{c}\cdot\mathbf{u})(\mathbf{u}\cdot\mathbf{u})\right] \tag{6}$$

The moving particles are allowed to move with five kinds of speed, c, $2c$, $3c$, $\sqrt{2}c$ and $2\sqrt{2}c$, as shown in Table 1.

In the present study, integrating Eq. (6) with respect to time and using the second order Runge-Kutta method lead to the following discretized equations in x-direction as

$$f_i^{n+\frac{1}{2}} = f_i^n + \frac{1}{2}\Delta t\left[-c_{i\alpha}\frac{\partial f_i^n}{\partial x_\alpha} + ac_{i\alpha}\frac{\partial}{\partial x_\alpha}\frac{f_i^n - f_i^{(0)n}}{\phi} - \frac{1}{\phi}\left(f_i^n - f_i^{(0)n}\right)\right]$$

$$f_i^n = f_i^n + \Delta t\left[-c_{i\alpha}\frac{\partial f_i^{n+\frac{1}{2}}}{\partial x_\alpha} + ac_{i\alpha}\frac{\partial}{\partial x_\alpha}\frac{f_i^{n+\frac{1}{2}} - f_i^{(0)n+\frac{1}{2}}}{\phi} - \frac{1}{\phi}\left(f_i^{n+\frac{1}{2}} - f_i^{(0)n+\frac{1}{2}}\right)\right] \tag{7a,b}$$

and the third-order upwind finite-difference scheme to discretize the spatial derivatives is used as

$$c_x\frac{\partial f}{\partial x} = c_x\frac{f(x-2\Delta x,y)-6f(x-\Delta x,y)+3f(x,y)+2f(x+\Delta x,y)}{6\Delta x} \quad (c_x>0)$$

$$c_x\frac{\partial f}{\partial x} = c_x\frac{-f(x+2\Delta x,y)+6f(x+\Delta x,y)-3f(x,y)-2f(x-\Delta x,y)}{6\Delta x} \quad (c_x<0) \tag{8a,b}$$

2.2 Model of flexible specific heat ratio

Most models in LBM are for incompressible fluids due to its simplicity of the structure, and only a few simulations by the models for compressible or thermal-fluid model have been reported (Alexander et al. 1993; Chen et al. 1994; Tsutahara and Kang 2002). In LBM, the mode of the fluid particle is limited to that due to translation. The ratio of the specific heats γ, then, is $\gamma=(D+2)/D$ and D represents the space dimension. For the case of two-dimensional, the ratio of specific heats is $\gamma=2.0$, and it will apply to monatomic gases only but not to the most important diatomic gas such as air.

The modified model (Kang et al. 2006) having energy modes except the translation $G_i(\mathbf{r},t)=f_i(\mathbf{r},t)E_i(\mathbf{r},t)$ to give the particle internal degree of freedom, which was originally proposed by Takada and Tsutahara (1999) in LBM, is introduce in the simulation. The distribution function $G_i(\mathbf{r},t)$ is assumed to approach by collision to its local equilibrium state $G_i^{(0)}(\mathbf{r},t)$ as the particle distribution functions do, and the evolution of $G_i(\mathbf{r},t)$ will be similar to Eq. (5) is transformed as follows:

$$\frac{\partial G_i}{\partial t} + c_{i\alpha}\frac{\partial G_i}{\partial x_\alpha} - ac_{i\alpha}\frac{\partial}{\partial x_\alpha}\frac{G_i - G_i^{(0)}}{\phi} = -\frac{1}{\phi}\left(G_i - G_i^{(0)}\right) \tag{9}$$

In this model, the motion of the particles is calculated by Eq. (5), and the local equilibrium distribution function is assumed to be given as the conventional form of Eq. (6). Here, assumed that all the particles at the local equilibrium stage have the same rotational energy. Then the expression for the ratio of the specific heats γ is written as

$$\gamma = \frac{D+2}{D'} = \frac{D+D_E+2}{D+D_E} \tag{10}$$

where D is the total degree of freedom of the particle motion and D_E is the degree of freedom of the rotation. The energy at the equilibrium stage E is expressed as

$$E = \frac{D}{2}\left(\frac{D+2}{D} - \gamma\right)e \tag{11}$$

$$G_i^{(0)} = Ef_i^{(0)} \tag{12}$$

When the flow is two-dimensional $D=2$ and the degree of freedom of the rotation $D_E=1$, for example, the energy E will be $E=e/3$ and other energy $2e/3$ will be distributed to the translation modes, and then each translation energy is $e/3$. The energy, therefore, is equally distributed to each degree of freedom of motion, and γ can be freely variable as follows.

$$1.0 < \gamma \le \frac{D+2}{D} \tag{13}$$

3 Analysis of the self-sustained oscillations

3.1 Numerical conditions

The edgetone configurations considered consist of sharp edge tip located in the medial plane of a fully developed two-dimensional jet as shown in Figure 2 ($w/d=9.0$). The primary regions of interest in an edgetone configuration are the vicinity of the nozzle and the wedge tip. The characteristic distances are the nozzle-wedge spacing or stand-off distance, w, and the height of the nozzle (or slit), d. The angle of wedge, α, is another significant parameter. The height of the nozzle and the wedge shape are similar to those of Brown's work (1937) and Bamberger's ones (2004). The nozzle height d of the models is 1(mm) and all the length scales are normalized by the nozzle height. Computational domains are set for $-10d \le x \le (132d \sim 141d)$ and $-120d \le y \le 140d$ for each case, and the wedge angles are composed of $\alpha = 20^0$ (case I) and $\alpha = 23^0$ (case II), respectively, which are clustered at the wedge. A parabolic inflow profile for the velocity is given on the inflow boundary. For spatial derivative s, a third-order-accurate up-wind scheme (second order accurate at the boundary) is employed and a second-order-accurate Runge-Kutta scheme is used for time integration. Adiabatic and no-slip conditions are employed on the wedge and wall surfaces, and an outflow condition is imposed on the outer far field boundary. A non-dimensional pressure fluctuation is given by:

$$\Delta p = \frac{p - p_0}{p_0} \tag{14}$$

Table 2 also shows the calculation conditions for each case. Computations start with a velocity $u_i(T(=Ut/d)=0) = (U_0,0)$ at the nozzle inlet.

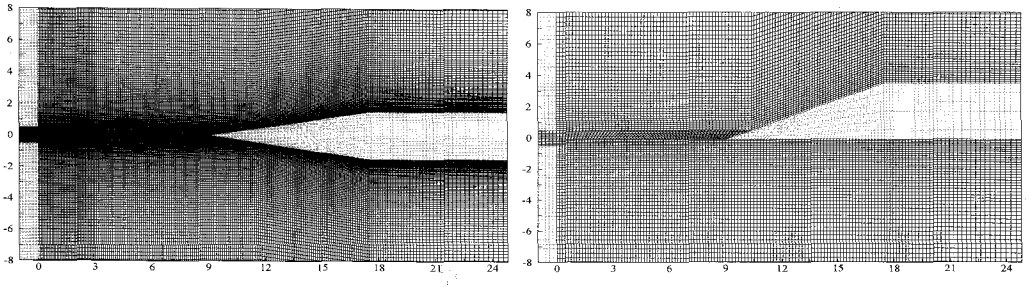

(a) case I (b) case II

Figure 2: Computational grid for each case ($w/d = 9.0$, enlarged)

Table 2: Calculation conditions

	w/d	Cells	Domains	Variables
Case I	3d	331×381	$-10d \le x \le 132d$ $-120d \le y \le 120d$	Re=250～600 ΔT =0.01 γ =1.4 20℃ air
	6d	361×381	$-10d \le x \le 135d$ $-120d \le y \le 120d$	
	9d	397×381	$-10d \le x \le 138d$ $-120d \le y \le 120d$	
	12d	433×381	$-10d \le x \le 141d$ $-120d \le y \le 120d$	
Case II	3d	266×301	$-10d \le x \le 132d$ $-120d \le y \le 120d$	
	6d	301×301	$-10d \le x \le 135d$ $-120d \le y \le 120d$	
	9d	321×301	$-10d \le x \le 138d$ $-120d \le y \le 120d$	
	12d	341×301	$-10d \le x \le 141d$ $-120d \le y \le 120d$	

3.2 Feedback loop

In the near-field flow structure, the formation, growth, transport and dissipation of vortices can be explained through a sequence of streamline plots. Figures 3 and 4 present a set of two streamline diagrams for two different cases with $w/d = 6.0$. The initial values are given at $U_0 = 12$ m/s, Re=600 and $\gamma = 1.4$. As shown in the figures, a vortex above the right-bound jet is counter clockwise and one below it is clock-wise due to their relative locations with respect to the jet. Initially, in Figures 3(a) and 4(a), the clock-wise vortex (arrows) under the wedge pulls the flow away from the lower side of the wedge apex. This jet motion causes the flow to impinge at the upper side of the wedge apex. Consequently, a high pressure center builds up at the upper side of the apex. The sense of the pressure dipole is pointed downwards. An acoustic wave from the pressure dipole has propagated outwards and specifically causes a low pressure center and a new vortex to appear at the lower corner of the nozzle exit. The vortex-acoustic coupling is further clarified. Initially at

$T = 0$, the dipole configuration is such that the pressure at the lower side of the wedge apex is at a minimum and the upper side of the wedge apex at a maximum. The acoustic feedback causes the pressure fields at the nozzle exit have the same sense, that is, high at the upper lip and low in the lower of the nozzle as it lags only slightly in phase.

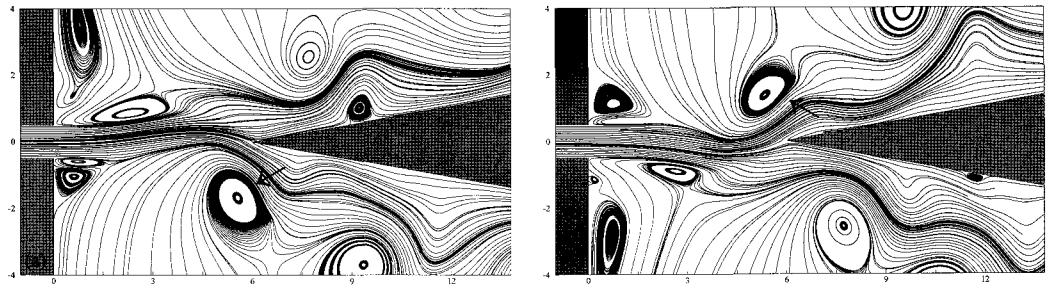

Figure 3: Time sequence of streamlines for case I ($w/d = 6.0$). (a) T=452, (b) T=459.

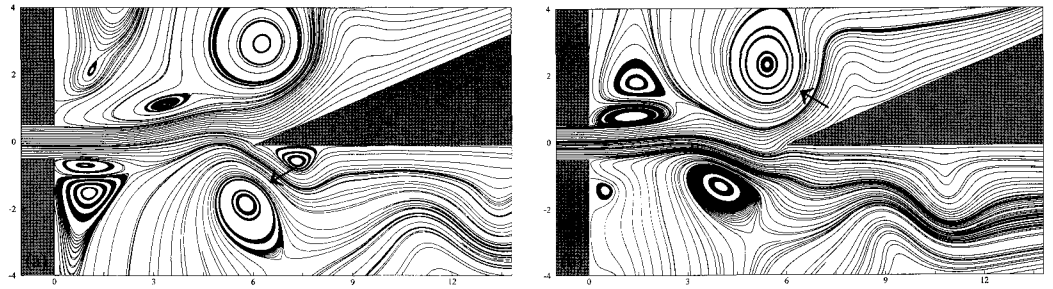

Figure 4: Time sequence of streamlines for case II ($w/d = 6.0$). (a) T=462, (b) T=469.

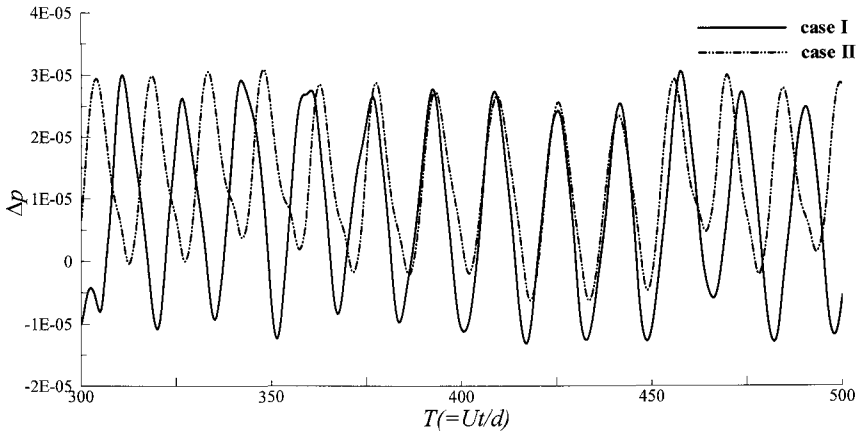

Figure 5: Time variation of acoustic pressure measured at $(100d,100d)$.

Since the velocity gradients at the lips are high, vortices quickly form at the nozzle exits when the pressure distribution changes. The pressure force causes the flow at the lower lip to bend up. Eventually, the roll-up movement develops into a new vortex. This new clockwise vortex gains energy from the jet and moves downstream, and at this moment, in Figures 3(b) and 4(b), a counter clockwise vortex (arrows) rolls above the wedge and

causes a high speed and low pressure region at the upper side of the wedge. This changed influence of the pressure differential across the wedge will soon be felt at the corners of the nozzle exit. The pressure field at the nozzle lips will be high at the lower corner and low at the upper corner according to the sense of the dipole pressure at the wedge apex. There is approximately 180 degree phase shift between the diagram 3(a), 4(a) and 3(b), 4(b). As a result, downstream, the alternating impingement of the vortices on the wedge creates a flow/structural system acting as an acoustic dipole. This acoustic energy propagates back upstream to organize and enhance flow instability at the jet orifice, further strengthening the alternate vortex shedding pattern developing at the nozzle exit. As the vortex shedding frequency matches phase with the acoustic frequency of the wedge dipole, an audible edge tone develops.

The time variations of the acoustic pressure measured at ($100d$,$100d$) in the x and y direction are shown in Figure 5 for the case of U_0 = 12 m/s. The observing point is radically considered on the edge tip (x_0, y_0). The solid line is case I and, and the dotted one is case II, respectively, and the sound signals fluctuate with a period of $\Delta T(= ut/d) = 15.38$ in case I and 14.71 in case II, which correspond to $S_t(= fd/u)$ = 0.065 and 0.068 at the first frequency level, respectively. The acoustic pressure becomes periodic with maxima and minima occurring at points. Moreover, it can be confirmed that the amplitude of the fluctuations of the acoustic pressure in the points is about 0.00003, and it has a more minute value than the pressure fluctuation at the vicinity of the edge with ± 0.00015.

3.3 Geometric parameter effects

In this section the geometric effects of stand-off distance between the nozzle outlet and the wedge for w/d = 3, 6, 9 and 12, respectively, is discussed. Initial conditions are set M = 0.2, Re=800 and γ = 1.4, respectively and all calculation conditions are the same in the case of the previous section.

Figures 6(a) through (d) and 7(a) through (d) show the instantaneous vorticity fields at T=460 for each case. According to Brown (1937) and Dougherty et al. (1994), when the distance from the wedge to the nozzle exit is less than w/d = 3.0, there is inadequate room for the jet to bend

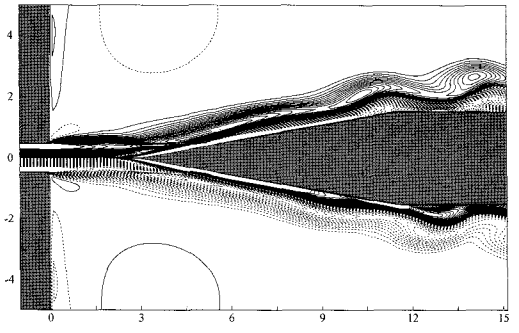

(a) w/d=3.0

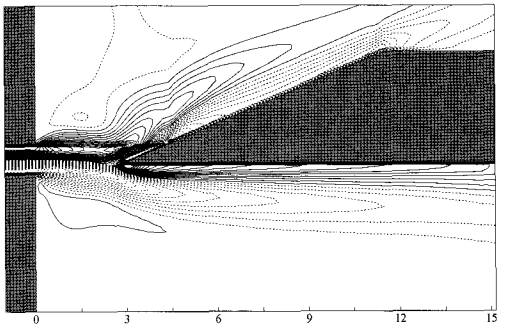

(a) w/d=3.0

(continued)

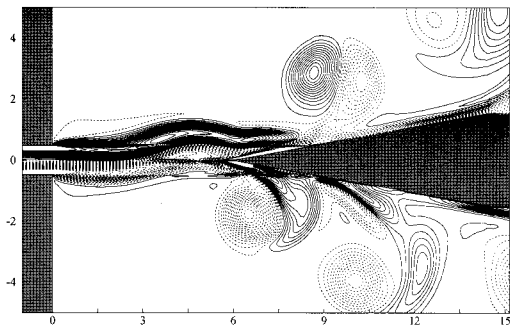

(b) w/d=6.0

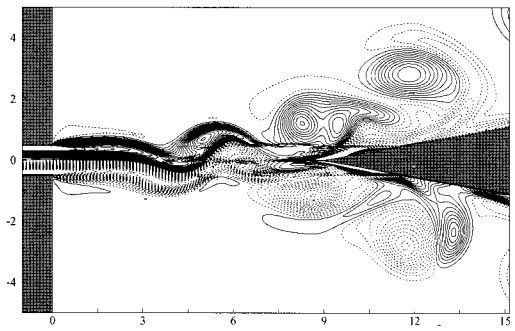

(c) w/d=9.0

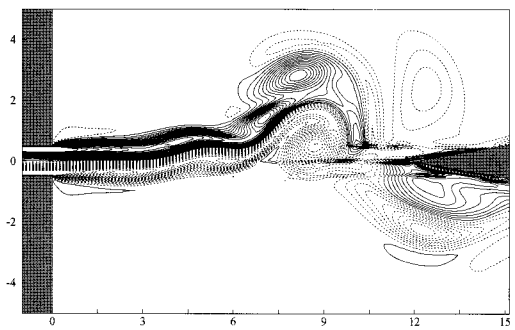

(d) w/d=12.0

Figure 6: Instantaneous vortex distribution of computational results under various w/d for case I; θ=20[deg].

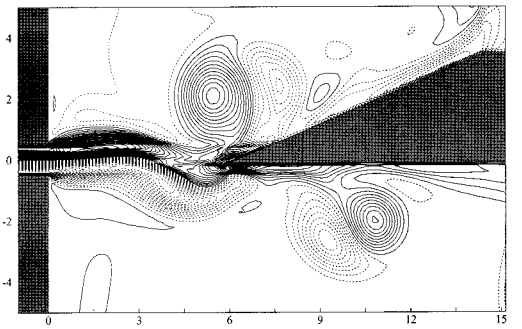

(b) w/d=6.0

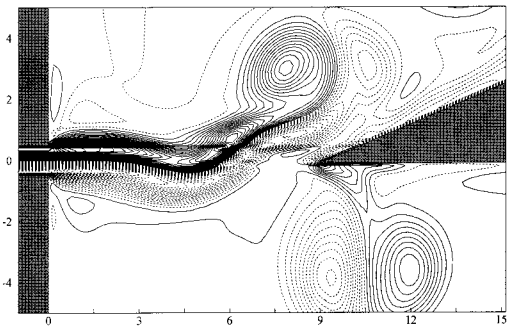

(c) w/d=9.0

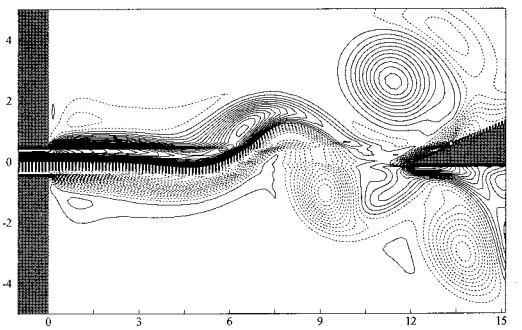

(d) w/d=12.0

Figure 7: Instantaneous vortex distribution of computational results under various w/d for case II; θ=23[deg].

To examine the farfield acoustic pressure for the case of M=0.2, Re=600 and $\gamma = 1.4$, Figures 8 and 9 show the acoustic pressure field for two $w/d = 6.0$ and 12.0 at $T(= ut/d) =$ 268, where the contour level Δp_{step} fluctuates from –0.001 to 0.0016. As can be seen in these figures, rarefaction waves with negative Δp and compression waves with positive Δp are generated alternately around the edge tip at the origin, and propagate symmetrically in the upper and lower parts of the wedge.

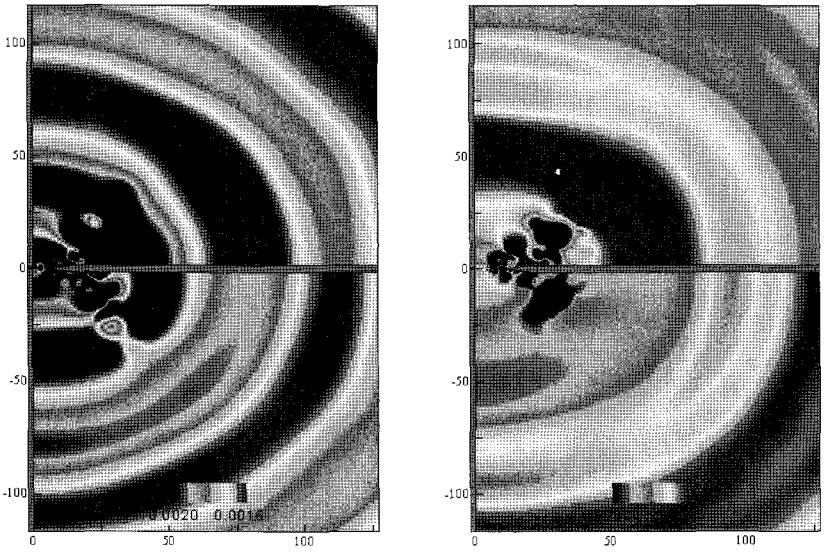

(a) w/d=6.0 (b) w/d=12.0

Figure 8: Acoustic pressure distribution for case I $(-0.002 \le \Delta p \le 0.0016)$.

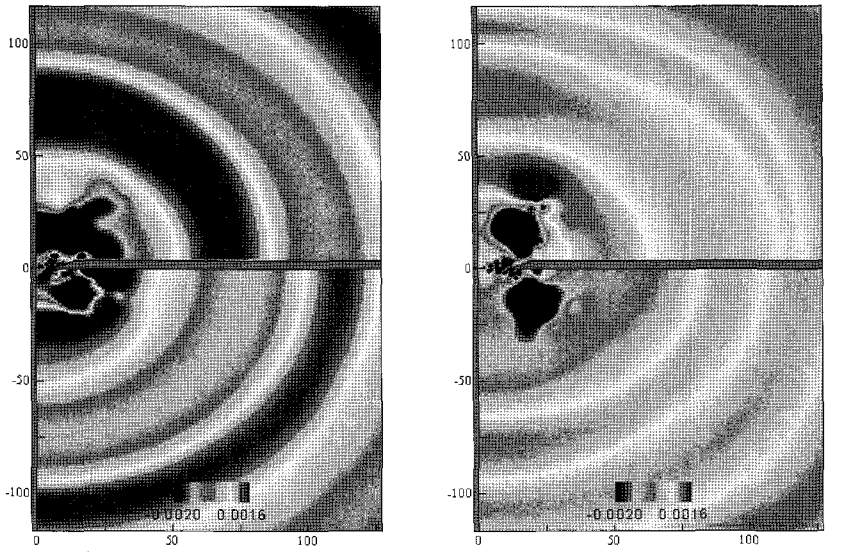

(a) w/d=6.0 (b) w/d=12.0

Figure 9: Acoustic pressure distribution for case II $(-0.002 \le \Delta p \le 0.0016)$.

Moreover, in case of $w/d = 12.0$, Figure 10 presents the acoustic signal measured at $(x, y) = (100d, \pm 100d)$ from the tip of the edge. In these figures when jet speed decreases as wedge distance increases, the jet is more susceptible to the wedge dipole effects, which deflect the jet and create vortex/undulation centers along the jet boundaries. Consequently, the jet-wedge interaction is weak and the jet exhibits the extremely dynamic nature of the edgetone flow field near the wedge apex. According to Brown's experiment (1937), when the distance from the wedge to nozzle exit is greater than $w/d = 20$, the acoustic feedback,

with strength decreasing linearly with distance, would be too weak to trigger alternate vortex shedding at the nozzle exit.

3.4 Evaluation and comparison

The Strouhal numbers S_t are presented in Figure 11 as a function of ratio w/d. Present simulations by analyzing the time evolution of the far-field pressure, deal with moderate Reynolds number, Re =250~600. Hence, the situation $n \approx 1$ is expected and the flow considered remains laminar. The three values of the stand-off distance w for 6, 9 and 12mm are evaluated, and the results obtained at the first frequency level $k = 1$ are reported. The present computations are compared to the experimental and numerical ones obtained previously in similar flow configurations by Brown (1937), Nyborg (1954), Bamberger et al. (2004), and Devillers & Coutier-Delgosha (2005). The theoretical law proposed by Holger, et al. (1977), Eq. (4) with $C = 0.92(k + 0.4)$, is also plotted in Figure 11 for frequency stages $k = 1$ and 2. The empirical law presented recently by Bamberger et al. (2004), Eq. (4) with $n = 1$ and $C = 0.495$, is also plotted for frequency level $k = 1$. In present results, the reliable agreement is found between experimental, numerical and theoretical results concerning the Strouhal numbers S_t. The discrepancies observed for both levels with the theoretical law proposed by Holger et al. (1977) were already reported by Howe (1998).

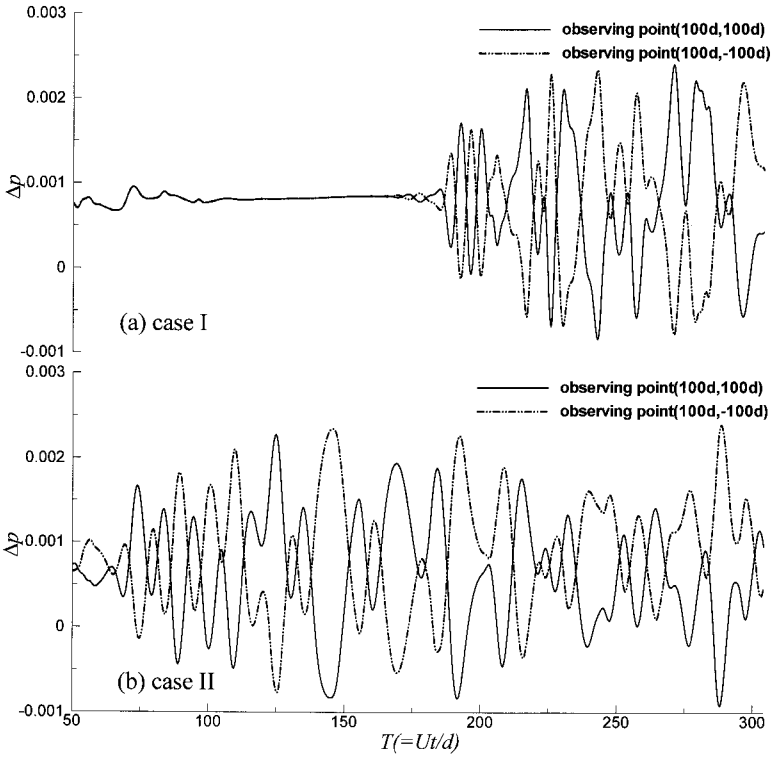

Figure 10: Characteristics of acoustic pressure for w/d = 12.0: Re=600, M=0.2.

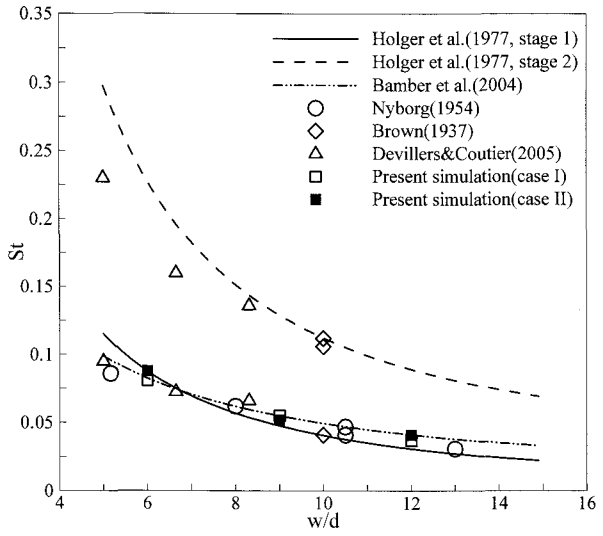

Figure 11: Comparison of the Strouhal numbers S_t with theoretical, numerical and experimental results of the literature (frequency stages 1 and 2).

Conclusions

The geometric effects of stand-off distance between the nozzle exit and the wedge for $w/d = 3.0$, 6.0, 9.0 and 12.0, respectively, are investigated to verify the feedback loop of edgetone using lattice Boltzmann model with 21 velocity bits, which is introduced the flexible heat ratio γ to simulate diatomic gases like air. Two-dimensional edgetone phenomenon with an angle of 20 degrees (for symmetric wedge) and an angle of 23 degrees (for inclined wedge) is successfully simulated by the applied FDLB model, and obtained results are as follows

1) With even very low Mach number flows (Ma$\leq$ 0.2), the present code can correctly predict the frequency characteristics of the discrete oscillation of a jet-edge feedback cycle for various inflow conditions.
2) When the distance from the wedge to the nozzle exit is less than $w/d = 3.0$, there is inadequate room for the jet to blend and the flow splits more or evenly on each side of the edge, and the edgetone, therefore, does not occur.
3) For the case of $w/d = 6.0$, the jet oscillates in periodic fashion, while the cases over $w/d = 9.0$, the jet also oscillate but the flow patterns do not show periodicity. According to Brown's work, when the stand-off distance is greater than $w/d = 20.0$, the acoustic feedback, with strength decreasing linearly with distance, would be too week to trigger alternate vortex shedding at the nozzle exit, and the present results are qualitatively agreement with previous works.

The results presented in this study show potentiality of finite-based LBM of flow-induced noises generated from the ventilating systems of vessel.

References

Alexander, F.J., S. Chen and D.J. Sterling. 1993. Lattice Boltzmann Thermodynamics. Physical Review E, **47**, 2249-2252.

Bamberger, A., E. Bansch and K.G. Siebert. 2004. Experimental and Numerical Investigation of Edge Tones. ZAMM-Journal of Applied Mathematics and Mechanics, **84**, **9**, 632-646.

Brown, G.B. 1937. The Vortex Motion Causing Edge Tones. Proceedings of the Physical Society of London, **49**, 493-507.

Buick, J.M., C.L. Buckley, C.A. Greated and J. Gilbert. 2000. Lattice Boltzmann BGK Simulation of Nonlinear Sound Waves: the Development of a Shock Front. Journal of Physics A, **33**, 3917-3928.

Chen, Y. and G.D. Doolen. 1998. Lattice Boltzmann Method for Fluid Flows. Annual Review Fluid Mechanics, **30**, 329-364.

Chen, Y., H. Ohashi and M. Akiyama. 1994. Thermal Lattice Bhatnager-Gross-Krook Model without Nonlinear Deviation in Macrodynamic Equations. Physical Review E, **50**, 2776-2783.

Devillers, J.F. and O. Coutier-Delgosha. 2005. Influence of the Nature of the Gas in the Edge-Tone Phenomenon. Journal of Fluids and Structures, **21**, 133-149.

Dougherty, N.S., B.L. Lin and J.M. O'Farrell. 1994. Numerical Simulation of the Edge Tone Phenomenon, NASA Contractor 4581.

Haydock, D. and J. Yeomans. 2001. Lattice Boltzmann Simulations of Acoustic Streaming, Journal of Physics A, **34**, 5201-5213.

Holger, D.K., T.A. Wilson and G.S. Beavers. 1977. Fluid Mechanics of the Edgetone. Journal of Acoustical Society of America, **62**, **5**, 1116-1128.

Howe, M.S. 1998. Acoustics of Fluid Structure Interaction. Cambridge University Press, Cambridge.

Inoue, O. and N. Hatakeyama. 2002. Sound Generation by a Two-dimensional Circular Cylinder in a Uniform Flow. Journal of Fluid Mechanics, **471**, 285-314.

Kang, H.K., S.W. Ahn and J.W. Kim. 2006. Application of the Internal Degree of Freedom to 3D FDLB Model and Simulations of Aero-acoustic. Journal of the Society of Naval Architects of Korea, **43**, **5**, 586-596.

Kang, H.K. and M. Tsutahara. 2007. An Application of the Finite Difference-based Lattice Boltzmann Model to Simulating Flow-Induced Noise. International Journal for Numerical Methods in Fluids, **53**, 629-650.

Lesieur, M. 1993. Turbulence in Fluids. Kluwer Academic Publisher, Dordrecht.

Nyborg, W.L. 1954. Self-maintained Oscillations of Jet in a Jet-edge System. I. Journal of the Acoustical Society of America, **26**, **2**, 174-182.

Powell, A. 1961. On the Edge Tone. Journal of Acoustical Society of America, **339**, 395-409.

Rossiter, J.E. 1962. The Effect of Cavities on the Buffeting of the Aircraft. Royal Aircraft Establishment Thecnical Memorandum 745.

Takada, N. and M. Tsutahara. 1999. Proposal of Lattice BGK Model with Internal Degrees of Freedom in Lattice Boltzmann Method. Transaction of JSME Journal B, **65**, **629**, 92-99.

Tsuchida, J., T. Fujisawa and G. Yagawa. 2006. Direct Numerical Simulation of Aerodynamic Sounds by a Compressible CFD Scheme with Node-by-node Finite Elements. Computer Methods in Applied Mechanics and Engineering, **195**, 1896-1910.

Tsutahara, M. and H. K. Kang. 2002. A Discrete Effect of the Thermal Lattice BGK Model. Journal of Statistical Physics, **107**, **1/2**, 479-498.

Wilde, A. 2004. Flow Acoustic Simulations Using the Lattice-Boltzmann Method. International Congress on FEM Technology with ANSYS & ICEM CFD Conference, Germany.

Wolfram, S. 1986. Cellular Automaton Fluids 1; Basic Theory. Journal of Statistical Physics, **45**, 471-526.